Journal of Magnetism and Magnetic Materials 113 (1992) 21–28
North-Holland

journal of magnetism and magnetic materials

Microstructure and magnetic properties of very thin CoCr films deposited on different underlayers by rf-sputtering

G. Pan, D.J. Mapps, M.A. Akhter

School of Electronic, Communication and Electrical Engineering, Polytechnic South West, Plymouth, Devon, PL4 8AA, UK

J.C. Lodder, P. ten Berge

Faculty of Electrical Engineering and Applied Physics, University of Twente, P.O. Box 217, 7500 AE Enschede, The Netherlands

H.Y. Wong and J.N. Chapman

Department of Physics and Astronomy, The University of Glasgow, Glasgow, G12 8QQ, UK

Very thin CoCr films deposited on different underlayers on glass disk substrates were studied by the magneto-optic Kerr effect, VSM, torque magnetometry and TEM selected area diffraction. Square or near square perpendicular loops were obtained from Co/Ti, CoCr/Au, CoCr/Al, CoCr/C and CoCr/Si films. TEM SAD study revealed that the crystalline structure is a key factor determining the magnetic anisotropy of the very thin CoCr films. In particular, the *c*-axis of the hcp CoCr films which exhibit square perpendicular loops is perpendicular to the film plane whilst that of the CoCr films which exhibit a thin and flat perpendicular loop lies in the film plane. The texture of the very thin CoCr films deposited on different underlayers is mainly dependent on the structure and texture of underlayers. The relation between the structure of CoCr and its underlayers is discussed.

1. Introduction

There is a considerable current interest in the effect of underlayers on the magnetic properties of both perpendicular and longitudinal magnetic recording media [1,2]. In a previous paper [1] we have reported on the magnetic properties of very thin CoCr films deposited on Ti underlayers. Very pronounced effects of Ti underlayers on the shearing and the squareness ratio of the perpendicular loops have been observed in such CoCr films. In order to understand the origin of the underlayer effect, further experimental investigation into the microstructure, micromagnetics and magnetic properties of these films have been undertaken. We report here on a detailed experimental programme of magnetic measurements together with microstructural examinations by TEM of the 160 Å thick CoCr films with different underlayers.

Correspondence to: Dr. G. Pan, School of Electronic, Communication and Electrical Engineering, Polytechnic South West, Plymouth, Devon, PL4 8AA, UK.

2. Experimental details

Very thin CoCr films were deposited on different underlayers or directly on to glass disk substrates. The film thickness was measured by a talystep and a Scanning Auger microprobe (SAM). The Cr content of the CoCr films is 23 at% by Auger. The magnetic properties of the CoCr films were studied using a magneto-optic Kerr effect (MOKE) system, a vibration sample magnetometer (VSM) and a torque magnetometer. The film structure and crystal orientation

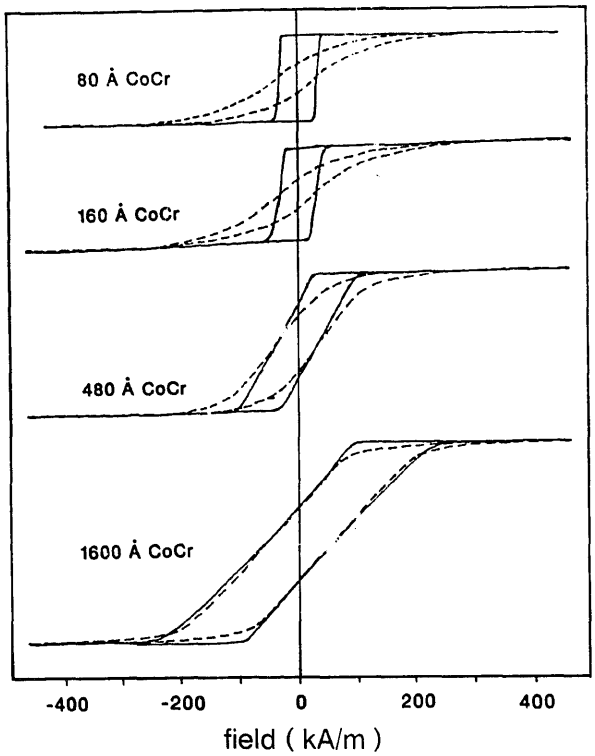

Fig. 1. Perpendicular MOKE loops of different thickness CoCr films with and without Ti underlayers (solid and dashed line respectively). Vertical axis is in arbitrary units.

were investigated by selected area diffraction (SAD) on a JEOL 2000FX TEM. For the preparation of TEM specimens, glass disk substrates were precoated with carbon films before the deposition of underlayers and the CoCr films themselves. The films were then floated off in water.

3. Results

3.1. Magnetic measurements

Fig. 1 shows the perpendicular MOKE loops of different thickness CoCr films with Ti underlayers (solid line) and without Ti underlayers (dashed line). For the 1600 Å thick CoCr films, the principal difference of the MOKE loops of CoCr films with and without Ti underlayers is only in the "shoulder" of the loop. As the CoCr film thickness reduces, the MOKE loops of the CoCr films deposited directly on glass become more rounded. On the other hand, the MOKE loops of CoCr films on Ti underlayers become steeper and squarer. The shearing of the perpendicular loops has been discussed in the light of a stripe domain model suggested by Weilinga and Lodder [3] and a particulate model suggested by Chang and Fredkin [1,4].

Fig. 2 shows the Ti underlayer thickness effect on the perpendicular loops of 160 Å thick CoCr films, which indicates that the squareness and the shearing of the loops are strongly affected by the existence of even a very thin Ti underlayer. The minimum Ti thickness to obtain a square loop is about 250 Å.

The perpendicular M–H loops of 160 Å thick CoCr films without Ti underlayer and with Ti underlayer were also measured by VSM and results are shown in fig. 3. The square VSM perpendicular loop for the 160 Å thick CoCr film on Ti and a thin and curved one for the films without Ti are in good agreement with the corre-

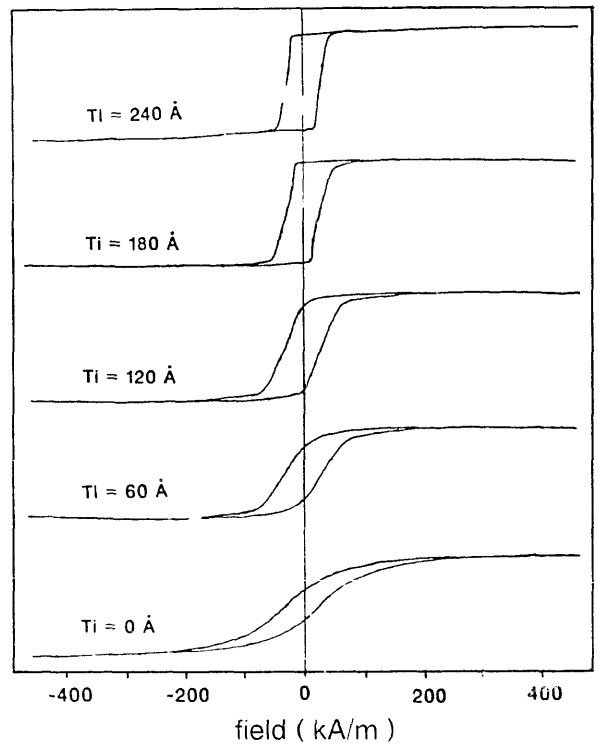

Fig. 2. Ti underlayer thickness effect on the perpendicular MOKE loops of 160 Å thick CoCr films. Vertical axis is in arbitrary units.

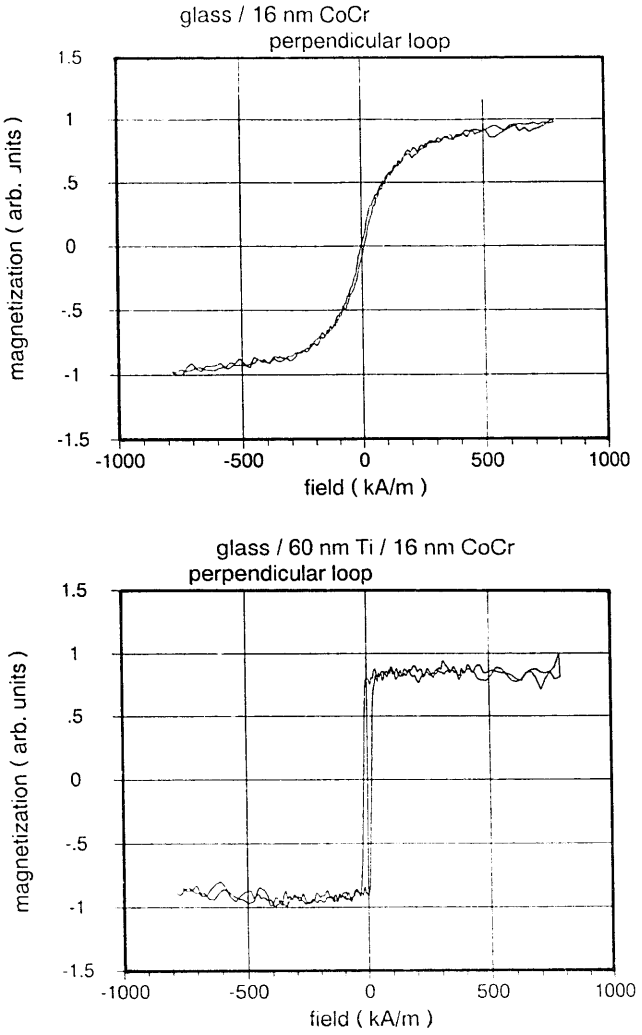

Fig. 3. $M-H$ loops of 160 Å thick CoCr films with and without Ti underlayers measured by VSM.

sponding MOKE loops, indicating an improved perpendicular easy axis behavior of the CoCr films gown on Ti underlayers.

Fig. 4 shows the torque magnetometer plots of the 160 Å thick CoCr films with and without Ti underlayers. Torque curves for both samples were initiated with the applied field in the plane of the sample. Under this condition, torque curves which start at zero degree with negative slope indicate an anisotropy perpendicular to the film plane and with a positive slope indicate an anisotropy in the plane of the films. As shown in fig. 4, the CoCr on glass exhibits a typical in-plane anisotropy torque curve, while the CoCr film on Ti exhibit a near perpendicular anisotropy torque curve. It is obvious that the magnetization easy axis of such thin CoCr film is dependent on the Ti underlayer.

Further experiment on the very thin CoCr films with other different underlayers was undertaken and fig. 5 shows the perpendicular MOKE loops of 80 Å thick CoCr films on different underlayers. Among them, the 80 Å thick CoCr films on Ti, Au, Al and C underlayers or directly deposited on Si substrate exhibit square or near square perpendicular MOKE loops. By contrast the CoCr film on a Cr underlayer exhibits a thin and flat perpendicular loop. The different height of the vertical axis of the loops is believed to be caused by the underlayer enhancement [5]. The effect of different underlayers on the magnetic properties of the initial growth layer of CoCr films can be clearly seen from this figure.

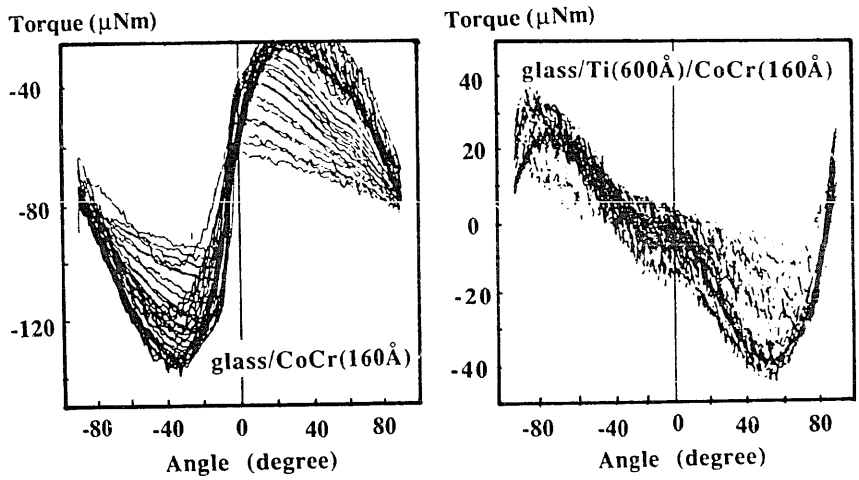

Fig. 4. Torque curves of 160 Å thick CoCr films with and without Ti underlayers.

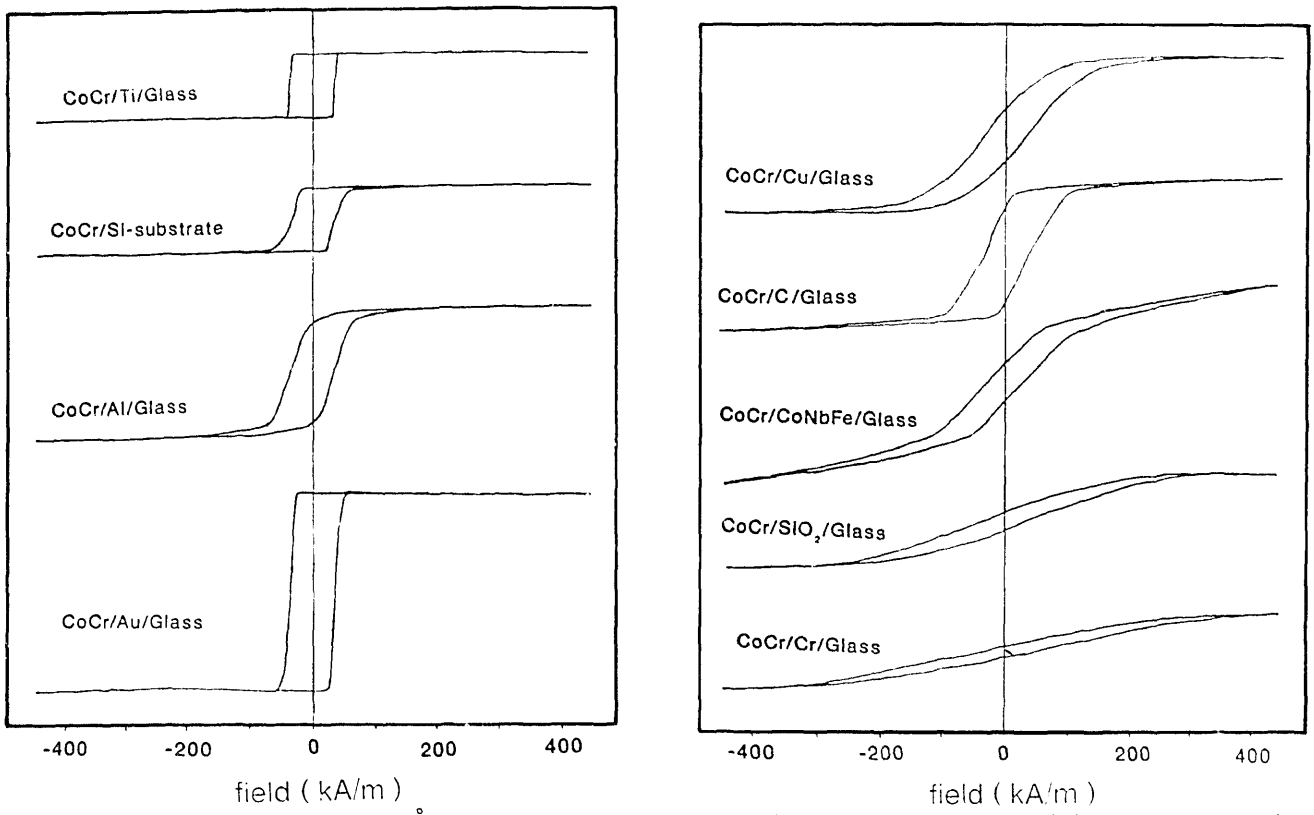

Fig. 5. Perpendicular MOKE loops of 80 Å thick CoCr films deposited on different underlayers, the Y axis is in arbitrary units, but in the same scaling.

3.2. Film microstructure and texture

In order to understand the structural origin of the underlayer effect, the CoCr films and their underlayers were studied by observing selected area diffraction (SAD) patterns with the specimen untilted and tilted through 30° on a JEOL 2000FX TEM.

Let us start with a brief review of the electron diffraction techniques for polycrystalline thin films [6]. In electron diffraction, only those planes which are near parallel to the incident electron beam contribute to the diffraction patterns because the Bragg angle in electron diffraction is very small (less than 1° or 2°).

Fig. 6a is a schematic drawing of a [00.1] oriented hcp Co crystal and the SAD pattern of the [00.1] textural hcp Co films. For such films, the main reflection rings are $(1\bar{1}00)$, $(11\bar{2}0)$, $(20\bar{2}0)$, ..., all of which are in the form of $\{hki0\}$. Reflection rings of (0002), $(01\bar{1}1)$, ..., $\{hkil\}$ $(l \neq 0)$ would not appear. When the specimen is tilted through 30°, the $\{hki0\}$ rings break into arcs along the diameter parallel to the tilting axis; along the perpendicular diameter, arcs such as $(01\bar{1}1)$ appear because this plane makes an angle of 28° with the c-axis. The schematic drawing of SAD patterns of the [11.0] and [10.0] textural Co films are shown in figs. 6b and c respectively. When we observe the SAD patterns of the [11.0] and [10.0] textural polycrystalline films with specimen tilted, it is very difficult to predict when arcs will occur for every family of planes because of the complex of angles within each family. However, one of the obvious features for such textural films is that the (0002) ring will break into arcs along the diameter parallel to the tilting axis.

The experimental results of the SAD patterns of 160 Å thick CoCr films on Ti, Cr, C and Cu underlayers with the specimen untilted and tilted

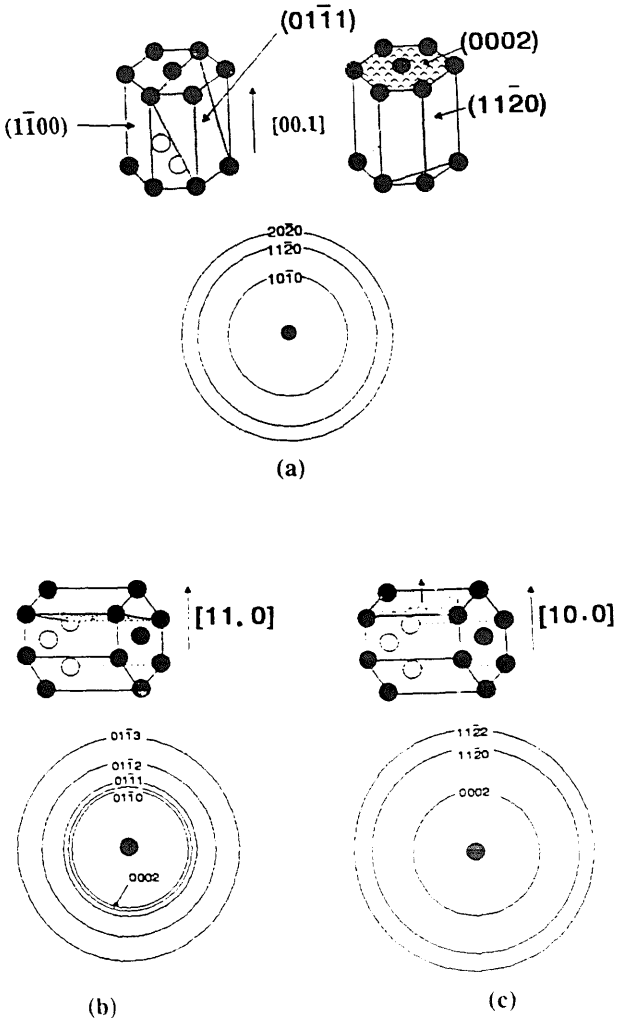

Fig. 6. Schematic drawing of (a) [00.1] zone axis SAD pattern, (b) [11.0] zone axis SAD pattern and (c) [10.0] zone axis SAD pattern of hcp Co polycrystalline films.

through 30° are shown in fig. 7. As mentioned above, these TEM specimens were deposited on a precoated C layers on glass substrates. However, MOKE measurement of these films showed similar loops to those shown in fig. 5. The SAD patterns are indexed in tables 1 to 4. If we examine figs. 6, 7 and tables 1 to 4 carefully, the following conclusions can be drawn.

The SAD patterns of the CoCr films on Ti and C underlayers with the specimen untilted and tilted are as expected from a strong [00.1] textural hcp films.The main reflection rings of the Co on both patterns are (1$\bar{1}$00), (11$\bar{2}$0) and (20$\bar{2}$0) when untilted. Diffraction rings of the form (000l), where $l \neq 0$, are not seen. When the specimen was tilted through 30°, the (1$\bar{1}$00), (11$\bar{2}$0) and (20$\bar{2}$0) rings are broken into arcs along the diameter parallel to the tilting axis. Arcs, such as (01$\bar{1}$1), appear along the perpendicular diameter. The c-axis of such films is perpendicular to the film plane.

The CoCr on Cr showed a mixed [11.0] and [10.0] zone axis patterns. When the specimen was tilted, the (0002) ring breaks into arcs. The c-axis of such films lies in the film plane. The CoCr on Cu has no texture. Reflection rings from all planes are present on the SAD patterns. When specimen was tilted, no changes to the pattern could be seen.

The underlayer structure can also be clarified from these patterns. The Ti underlayer has a

Table 1
Summary of SAD patterns of C/Ti(300 Å)/CoCr(160 Å) films with specimen untilted and tilted

Ring	Diameter	Plane spacing [Å]		Structure	*hkil*	Untilted	Tilted
		measured	ASTM				
1	29.0	2.544	2.555	Ti hcp	10$\bar{1}$0	medium ring	ring & arcs‖
2	31.5	2.342	2.342	Ti hcp	0002	medium ring	unchanged
3	32.9	2.242	2.243	Ti hcp	01$\bar{1}$1	very weak ring	strong arcs ⊥
4	34.0	2.170	2.170	Co hcp	10$\bar{1}$0	strong ring	strong arcs‖
5	38.5	1.916	1.915	Co hcp	01$\bar{1}$1	invisible	strong arcs ⊥
6	42.9	1.72	1.72	Ti hcp	01$\bar{1}$2	invisible	weak arcs ⊥
7	50.2	1.470	1.475	Ti hcp	11$\bar{2}$0	medium ring	medium arcs‖
8	55.2	1.337	1.332	Ti hcp	01$\bar{1}$3	very weak ring	unchanged
9	58.6	1.259	1.253	Co hcp	11$\bar{2}$0	strong ring	strong arcs‖
10	67.5	1.093	1.085	Co hcp	20$\bar{2}$0	very weak ring	weak ring & arcs‖

Table 2
Summary of SAD patterns of C/Cr(300 Å)/CoCr(160 Å) films with specimen untilted and tilted

Ring	Diameter	Plane spacing [Å]		Structure	*hkil*	Untilted	Tilted
		measured	ASTM				
1	34.0	2.170	2.170	Co hcp	$10\bar{1}0$	weak ring	unchanged
2	36.2	2.04	2.04	Cr bcc	011	strong ring	ring & arcs‖
3	36.2	2.038	2.035	Co hcp	0002	strong ring	ring & arcs‖
4	38.5	1.916	1.915	Co hcp	$01\bar{1}1$	strong ring	ring & arcs‖
5	49.8	1.481	1.484	Co hcp	$01\bar{1}2$	weak ring	weak arcs
6	51.0	1.447	1.443	Cr bcc	002	strong ring	strong arcs‖
7	58.6	1.259	1.253	Co hcp	$11\bar{2}0$	weak ring	unchanged
8	62.4	1.182	1.178	Cr bcc	112	weak ring	medium arcs ⊥
9	63.8	1.156	1.15	Co hcp	$01\bar{1}3$	weak ring	unchanged
10	69	1.07	1.067	Co hcp	$11\bar{2}2$	very weak ring	unchanged
11	72	1.02	1.02	Cr bcc	022	weak ring	ring & arcs‖

Table 3
Summary of SAD patterns of C/CoCr(160 Å) films with specimen untilted and tilted

Ring	Diameter	Plane spacing [Å]		Structure	*hkil*	Untilted	Tilted
		measured	ASTM				
1	27	2.17	2.17	Co hcp	$10\bar{1}0$	strong ring	strong arcs‖
2	28.8	2.034	2.035	Co hcp	0002	faint	faint
3	30.5	1.92	1.915	Co hcp	$01\bar{1}1$	faint	strong arcs ⊥
4	46.6	1.257	1.253	Co hcp	$11\bar{2}0$	strong ring	strong arcs‖
5	53.8	1.089	1.085	Co hcp	$20\bar{2}0$	medium ring	medium arcs‖
6	55	1.065	1.068	Co hcp	$11\bar{2}2$	faint	strong arcs ⊥
7	61.2	0.957	0.957	Co hcp	$02\bar{2}2$	invisable	weak arcs ⊥
8	71.6	0.818	0.82	Co hcp	$12\bar{3}0$	weak ring	medium arcs‖

Table 4
Summary of SAD patterns of C/Cu(300 Å)/CoCr(160 Å) films with specimen untilted and tilted

Ring	Diameter	Plane spacing [Å]		Structure	*hkil*	Untilted	Tilted
		measured	ASTM				
1	34.0	2.170	2.170	Co hcp	$10\bar{1}0$	weak ring	unchanged
2	35.3	2.09	2.087	Cu fcc	111	strong ring	unchanged
3	36.0	2.049	2.038	Co hcp	0002	medium ring	unchanged
4	38.5	1.916	1.915	Co hcp	$01\bar{1}1$	weak ring	unchanged
5	41.0	1.80	1.808	Cu fcc	002	medium ring	unchanged
6	57.8	1.276	1.278	Cu fcc	022	medium ring	unchanged
7	58.6	1.259	1.253	Co hcp	$11\bar{2}0$	medium ring	unchanged
8	68.0	1.085	1.085	Co hcp	$20\bar{2}0$	medium ring	unchanged
9	69.4	1.063	1.067	Co hcp	$11\bar{2}2$	weak ring	unchanged
10	71.0	1.039	1.044	Cu fcc	222	weak ring	unchanged

preferred hcp [00.1] texture. The C layer is amorphous. The Cr underlayer has a preferred bcc [100] texture. The Cu underlayer has a fcc structure with no texture. The correlation of the underlayer structure and the CoCr texture is schematically given in fig. 8.

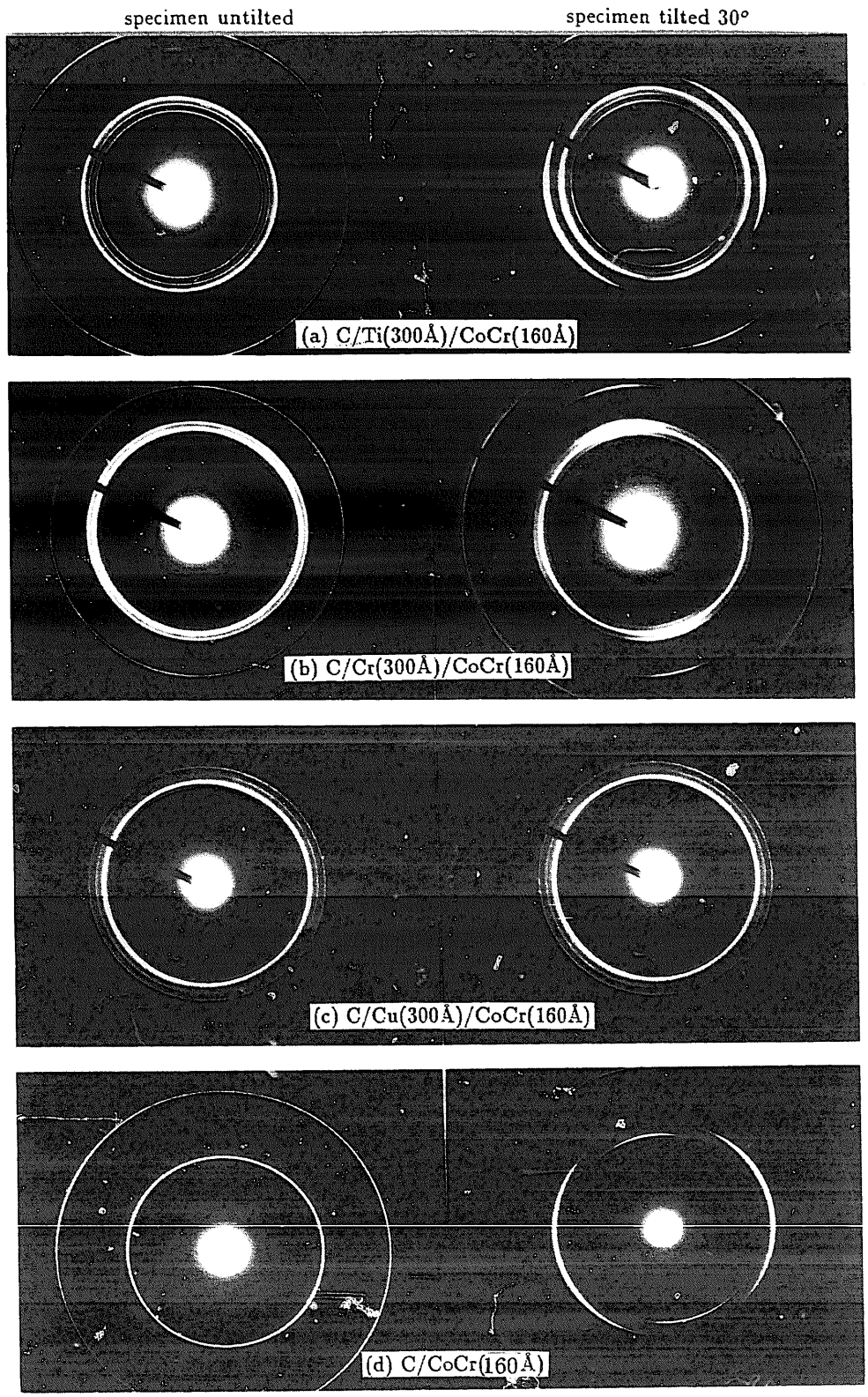

Fig. 7. SAD patterns of 160 Å thick CoCr films deposited on Ti, Cr, Cu and C underlayers.

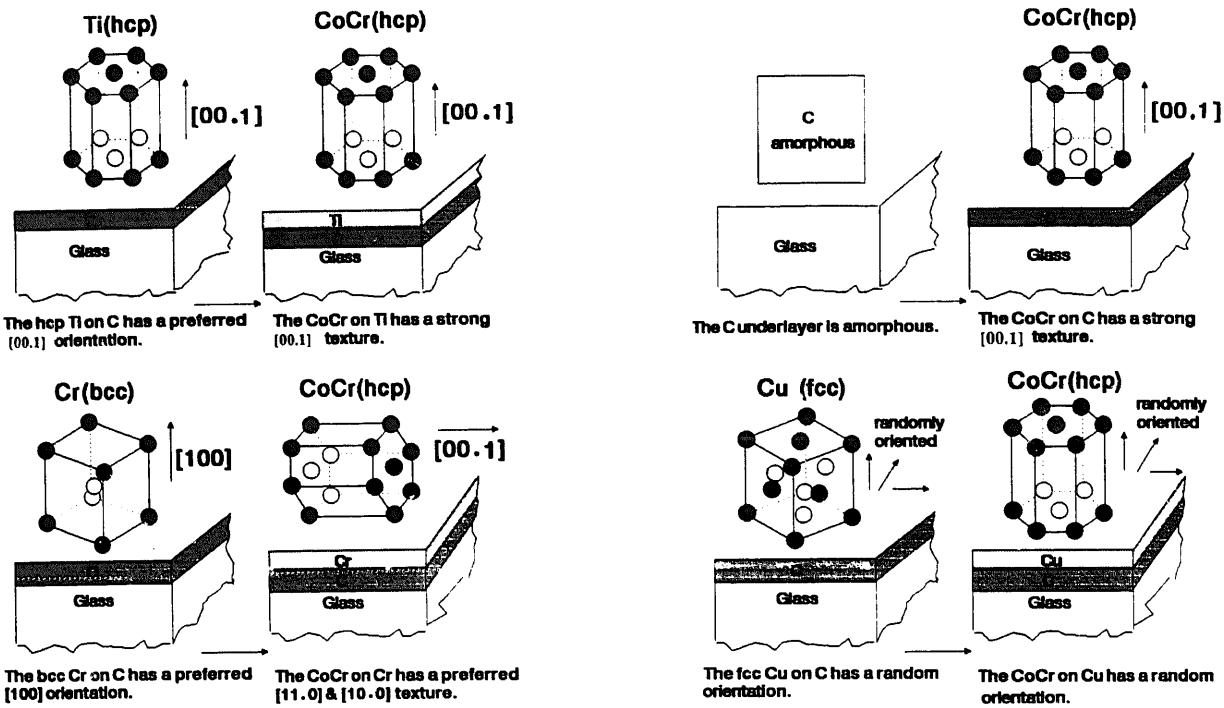

Fig. 8. Schematic representation of the effect of underlayer structure on the texture on CoCr films.

4. Discussion and conclusions

In summary, we conclude that the square or near square perpendicular loops of the very thin CoCr films originate from the improved perpendicular anisotropy of the films due to their growth on appropriate underlayers. Our TEM SAD study revealed that the microstructure is a key factor in determining the easy axis anisotropy of the very thin CoCr films. The c-axis of those hcp CoCr films which exhibit square perpendicular loops, such as CoCr/Ti and CoCr/C, are perpendicular to the film plane. The c-axis of the hcp CoCr films which exhibit poor perpendicular loops, such as CoCr/Cr, lies in the film plane.

The texture of the very thin CoCr films deposited on different underlayers is dominated by the structure and texture of the underlayers. The Ti underlayer which has a preferred hcp [00.1] texture encourages the hcp CoCr to grow epitaxially into a strong c-axis texture. The amorphous C is another suitable underlayer for the growth of [00.1] textural CoCr films.This may be explained by the fact that the CoCr film itself has the potential to grow into a c-axis texture because its (0002) plane has the lowest surface energy [2], and the amorphous C underlayer provides a free-growth substrate condition for the CoCr. The CoCr films on the [100] textural bcc Cr underlayer were forced to grow into a mixed [11.0] and [10.0] texture. This is perhaps due to the bcc [100] texture being more suitable for the epitaxial growth of hcp CoCr films with c-axis lying in the film plane.

References

[1] D.J. Mapps, M.A. Akhter and G. Pan, IEEE Trans. Magn. MAG-26 (1990) 1614.
[2] T. Yeh, J.M. Sivertsen and J.H. Judy, IEEE Trans. Magn. MAG-26 (1990) 1590.
[3] T. Wielingaa and J.C. Lodder, Phys. Stat. Sol. (a) 96 (1986) 255.
[4] Ching-Ray Chang and D.R. Fredkin, IEEE Trans. Magn. MAG-23 (1987) 2052.
[5] J. Zak, E.R. Moog, C. Liu and S.D. Bader, J. Magn. Magn. Mater. 89 (1990) 107.
[6] J.W. Edington, Electron diffraction in the electron microscope, Philips (1975).